

# AUGMENTATIONS AND RULINGS OF LEGENDRIAN KNOTS

JOSHUA M. SABLOFF

ABSTRACT. A connection between holomorphic and generating family invariants of Legendrian knots is established; namely, that the existence of a ruling (or decomposition) of a Legendrian knot is equivalent to the existence of an augmentation of its contact homology. This result was obtained independently and using different methods by Fuchs and Ishkhanov [12]. Close examination of the proof yields an algorithm for constructing a ruling given an augmentation. Finally, a condition for the existence of an augmentation in terms of the rotation number is obtained.

## 1. INTRODUCTION

A fundamental problem in Legendrian knot theory is to determine when two knots are (or are not) Legendrian isotopic.<sup>1</sup> Bennequin’s 1983 paper [1] started the enterprise by introducing the two “classical” invariants of Legendrian knots, the Thurston-Bennequin and rotation numbers. Classification results based on these invariants followed in the early 1990’s: Legendrian unknots [6], torus knots [9], and figure eight knots [9] are completely classified by their topological type and classical invariants.

Starting in the late 1990’s, two methods for constructing “non-classical” invariants of Legendrian knots were developed. The first is a relative version of the contact homology of Eliashberg, Givental, and Hofer [7]. This theory uses holomorphic techniques to associate a non-commutative differential graded algebra (DGA) to a knot diagram. The homology of the DGA is invariant under Legendrian isotopy. Chekanov rendered this theory combinatorially computable and used a linearized version of it to distinguish examples of Legendrian  $5_2$  knots in the standard contact  $\mathbb{R}^3$  that have the same classical invariants [2].<sup>2</sup> The second method is based on generating families, i.e. families of functions whose critical values generate fronts of Legendrian knots. Chekanov has produced “ruling” or “decomposition” invariants based on generating families that can distinguish his original  $5_2$  examples (see [3, 4]). In addition, Traynor has fashioned a non-classical theory based on generating families for Legendrian links in the solid torus [18].

---

<sup>1</sup>See Section 2 for all definitions relevant to the introduction.

<sup>2</sup>This invariant is also referred to as the Chekanov-Eliashberg DGA in the literature.

The goal of this paper is to strengthen a connection, discovered by Fuchs [11], between the ability to linearize the contact homology DGA and the non-vanishing of Chekanov’s count of rulings for Legendrian knots in the standard contact  $\mathbb{R}^3$ . It is possible to linearize the contact homology DGA if and only if there exists an augmentation, i.e. a map  $\varepsilon$  from the algebra to the base ring that sends the image of the differential to zero. It is useful to further stipulate that the augmentation vanishes on generators of nonzero grading; such an augmentation is called “graded”. Fuchs’ original result was:

**Theorem 1.1** (Fuchs [11]). *If a front diagram of a Legendrian knot  $K$  has a (graded) normal ruling, then the contact homology DGA of  $K$  has a (graded) augmentation.*

The central result of this paper is the converse, which Fuchs and Ishkhanov have proved independently, using different methods, in [12]:

**Theorem 1.2.** *If the contact homology DGA of a Legendrian knot  $K$  has a (graded) augmentation, then any front diagram of  $K$  has a (graded) normal ruling.*

A consequence is an easy criterion for checking if the contact homology DGA of a Legendrian knot has an augmentation:

**Theorem 1.3.** *If the Chekanov-Eliashberg DGA of a Legendrian knot  $K$  has an augmentation that vanishes on generators of odd degree, then its rotation number is zero.*

These results contribute to recent work that examines the relationship between the contact homology and generating family approaches to constructing non-classical invariants. Ng and Traynor found that a linearized version of the contact homology DGA and generating family homology contain the same information for a large class of two-component links in the solid torus [16]. Work of Zhu [19] and of Ekholm, Etnyre, and Sullivan [5] (see also [13]) shows that a different sort of generating function homology that uses “graph trees” for a single set of generating functions can be used to compute the contact homology DGA. The ideas behind this work have already provided the motivation for Ng’s combinatorial construction of invariants of topological braids and knots using the contact homology of Legendrian tori in  $ST^*S^3$  [15].

The rest of the paper is organized as follows: Section 2 lays out the necessary background and notation for diagrams of Legendrian knots, the contact homology DGA, and normal rulings. Section 3 contains the proof of Theorem 1.2 using a modification of a plat diagram of a Legendrian knot. Finally, the proof of Theorem 1.3 appears in Section 4.

**Acknowledgments.** This paper has greatly benefited from discussions with John Etnyre, Lisa Traynor, and especially Paul Melvin, who first conjectured Theorem 1.3 based on computations done by himself and Sumana Shrestha.

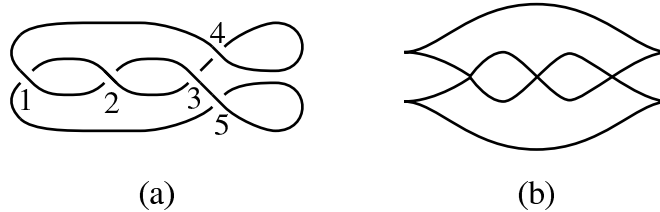


FIGURE 1. (a) Lagrangian and (b) front diagrams of a Legendrian trefoil knot. The meaning of the numbers in (a) will become clear in Section 2.2.

Conversations with Dmitry Fuchs helped to clarify the hypotheses in Theorem 1.3.

## 2. BACKGROUND NOTIONS

**2.1. Diagrams of Legendrian Knots.** This section briefly reviews the basic notions of Legendrian knot theory. For a more comprehensive introduction, see [8, 17].

The **standard contact structure** on  $\mathbb{R}^3$  is the completely non-integrable 2-plane field given by the kernel of  $\alpha = dz - y dx$ . A **Legendrian knot** is an embedding  $K : S^1 \rightarrow \mathbb{R}^3$  that is everywhere tangent to the contact planes. In particular, the embedding must satisfy

$$(1) \quad \alpha(K') = 0.$$

An ambient isotopy of  $K$  through Legendrian knots is a **Legendrian isotopy**.

As mentioned in the introduction, there are two “classical” invariants for Legendrian knots up to Legendrian isotopy. The first classical invariant is the **Thurston-Bennequin number**  $tb(K)$ , which measures the twisting of the contact planes around the knot  $K$ . The second classical invariant, the **rotation number**  $r(K)$ , is defined for *oriented* Legendrian knots. It measures the turning of the tangent direction to  $K$  inside the contact planes with respect to the trivialization given by the vector fields  $\partial_y$  and  $\partial_x + y\partial_z$ .

There are two useful projections of Legendrian knots. The **Lagrangian projection** is given by the map

$$\pi_l : (x, y, z) \mapsto (x, y),$$

while the **front projection** is given by

$$\pi_f : (x, y, z) \mapsto (x, z).$$

The Lagrangian and front projections of a Legendrian trefoil knot appear in Figure 1.

In the front projection, the  $y$  coordinate of a knot may be recovered from the slope of the front projection via (1):

$$(2) \quad y = \frac{dz}{dx}.$$

This fact has several consequences:

- The front projection of a Legendrian knot is never vertical. Instead of vertical tangencies, front projections have *cusps* like those on the extreme left and right of Figure 1(b).
- There is no need to specify crossing information at a double point: the strand with the smaller slope always has a smaller  $y$  coordinate. This means that it will pass in *front* of the strand with the larger slope, as the  $y$  axis must point into the page in the front projection.
- Any circle in the  $xz$  plane that has no vertical tangencies and that is immersed except at finitely many cusps lifts to a Legendrian knot via equation (2).

A front diagram is in **plat position** if all of the left cusps have the same  $x$  coordinate, all of the right cusps have the same  $x$  coordinate, and no two crossings have the same  $x$  coordinate. For example, the diagram of the trefoil in Figure 1(b) is in plat position. The  $x$  coordinates of the crossings and cusps are the **singular values** of the front. Any front diagram may be put into plat position using Legendrian versions of Reidemeister type II moves and planar isotopy.

Though the front projection is easier to work with, it is more natural to define the contact homology DGA using the Lagrangian projection. Ng's **morsification** procedure (see [14]) gives a canonical translation from a front diagram to a Lagrangian diagram. This procedure, in fact, was used to derive the Lagrangian projection in Figure 1(a) from the front projection in Figure 1(b). Combinatorially, there are three steps:

1. Smooth the left cusps;
2. Replace the right cusps with a loop (see the right side of the Lagrangian projection in Figure 1); and
3. Resolve the crossings so that the overcrossing strand is the one with smaller slope.

A key feature of the morsification procedure is that the heights of the crossings in the Lagrangian projection strictly increase from left to right, with the jumps in height between crossings as large as desired.

Finally, note that the rotation number of an oriented Legendrian knot  $K$  may be computed using the rotation number of the tangent vector to the Lagrangian projection in the plane. In the front projection, the rotation number is the difference between the number of downward-pointing cusps and the number of upward-pointing cusps.

**2.2. The Contact Homology DGA and Augmentations.** This section contains a brief review of the definition of the contact homology DGA of a

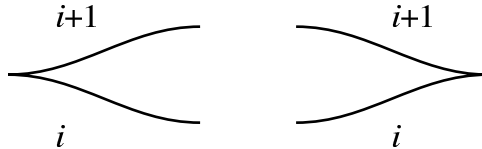


FIGURE 2. The function  $\mu$  must satisfy these relations near the cusps.

Legendrian knot. The DGA was originally defined by Chekanov in [2] for Lagrangian diagrams; see also [10].

Let  $K$  be an oriented Legendrian knot in the standard contact  $\mathbb{R}^3$  with a generic Lagrangian diagram  $\pi_l(K)$ . Label the crossings by  $q_1, \dots, q_n$ . Let  $\mathcal{A}$  be the graded free unital tensor algebra over  $\mathbb{Z}/2$  generated by the set  $\{q_1, \dots, q_n\}$ .<sup>3</sup> To define the grading, a capping path  $\gamma_i$  needs to be assigned to each crossing. A **capping path** is one of the two paths in  $\pi_l(K)$  that starts at the overcrossing of  $q_i$  and ends when  $\pi_l(K)$  first returns to  $q_i$ , necessarily at an undercrossing. Assume, without loss of generality, that the strands of  $\pi_l(K)$  at each crossing are orthogonal. The **grading** of  $q_i$  is:

$$|q_i| \equiv 2r(\gamma_i) - \frac{1}{2} \pmod{2r(K)}.$$

Extend the grading to all words in  $\mathcal{A}$  by letting the grading of a word be the sum of the gradings of its constituent generators.

*Remark.* It is simple to assign gradings directly from a plat diagram. Assign a grading of 1 to each generator coming from a right cusp. To assign a grading to a crossing, begin as in [3] by letting  $C(K)$  be the set of points on  $K$  corresponding to cusps of  $\pi_f(K)$ . The **Maslov index** is a locally constant function

$$\mu : K \setminus C(K) \rightarrow \mathbb{Z}/2r(K)$$

that satisfies the relations depicted in Figure 2 near the cusps. This function is well-defined up to an overall constant. Near a crossing  $q_i$ , let  $\alpha_i$  (resp.  $\beta_i$ ) be the strand of  $\pi_f(K)$  with more negative (resp. positive) slope. Assign the grading  $|q_i| = \mu(\alpha_i) - \mu(\beta_i)$ .

The next step is to define a differential on  $\mathcal{A}$  by counting certain immersions of the disk into  $\pi_l(K)$ . Label the corners of  $\pi_l(K)$  as in Figure 3(a). The immersions of interest are the following:

**Definition 2.1.** Given an ordered set of generators  $q_i, q_{j_1}, \dots, q_{j_k}$ , let  $\Delta(q_i; q_{j_1}, \dots, q_{j_k})$  be the set of orientation-preserving immersions

$$f : D^2 \rightarrow \mathbb{R}^2$$

that map  $\partial D^2$  to  $\pi_l(K)$  (up to smooth reparametrization), with the property that the restriction of  $f$  to the boundary is an immersion except at the points

<sup>3</sup>It is possible to define the algebra over  $\mathbb{Z}[T, T^{-1}]$ ; see [10].

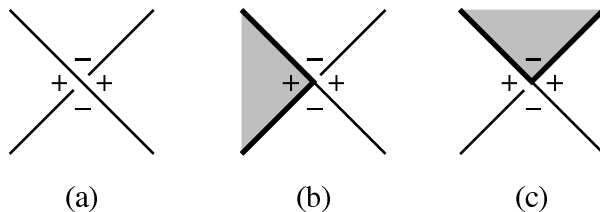


FIGURE 3. (a) A labeling of the quadrants surrounding a crossing; (b) The image of  $f \in \Delta(\dots)$  near the crossing  $q_i$  (the other + quadrant is also possible); (c) The image of  $f$  near the crossing  $q_{j_i}$  (the other - quadrant is also possible).

$q_i, q_{j_1}, \dots, q_{j_k}$  and these points are encountered in counter-clockwise order along the boundary. In a neighborhood of the points  $q_i, q_{j_1}, \dots, q_{j_k}$ , the image of the disk under  $f$  has the form indicated in Figure 3(b).

Finally, define the differential as follows:

**Definition 2.2.** The differential  $\partial$  is defined on a generator  $q_i$  by the formula:

$$(3) \quad \partial q_i = \sum_{\Delta(q_i; q_{j_1}, \dots, q_{j_k})} \#(\Delta(q_i; q_{j_1}, \dots, q_{j_k})) q_{j_1} \cdots q_{j_k},$$

where  $\#\Delta(\dots)$  is the number of elements in the set  $\Delta(\dots)$ , counted modulo 2. Extend  $\partial$  to all of  $\mathcal{A}$  via linearity and the Leibniz rule.

Note that the sum in the definition of  $\partial$  is finite, and that if  $\Delta(q_i; q_{j_1}, \dots, q_{j_k})$  is nonempty, then the height of the crossing at  $q_i$  is greater than the sum of the heights of the crossings  $q_{j_i}$ ; see [2].

*Remark.* In a diagram coming from the morsification of a plat diagram, the disks in the differential take on a simple form:

1. The disks are embedded, and
2. The intersection of any vertical line with a disk is connected.

*Example.* Number the crossings of the trefoil knot as in Figure 1. The first three crossings have grading 0, whereas the crossings that come from cusps in the plat diagram have grading 1. The only nontrivial differentials are:

$$\begin{aligned} \partial q_4 &= 1 + q_1 + q_3 + q_1 q_2 q_3, \\ \partial q_5 &= 1 + q_1 + q_3 + q_3 q_2 q_1. \end{aligned}$$

The central results in this theory are:

**Theorem 2.3** ([2]).

1. The differential  $\partial$  has degree  $-1$ .
2. The differential satisfies  $\partial^2 = 0$ .
3. The “stable tame isomorphism class” of the DGA is invariant under Legendrian isotopy.

The “stable” in part (3) of the theorem comes from the following operation on a DGA  $(\mathcal{A}, \partial)$ : the **degree  $i$  stabilization**  $S_i(\mathcal{A}, \partial)$  adds two new generators  $\beta$  and  $\alpha$  to the algebra, where

$$|\beta| = i \text{ and } |\alpha| = i - 1,$$

and the differential is extended to the new generators by:

$$\partial\beta = \alpha \text{ and } \partial\alpha = 0.$$

For the purposes of this paper, a stable tame isomorphism between two DGAs  $(\mathcal{A}, \partial)$  and  $(\mathcal{A}', \partial')$  is a DGA isomorphism

$$\psi : S_{i_1}(\cdots S_{i_m}(\mathcal{A})\cdots) \rightarrow S'_{j_1}(\cdots S'_{j_n}(\mathcal{A}')\cdots).$$

It is not easy to use the DGA to distinguish between Legendrian knots, as it — and its homology — are fairly complicated objects. Chekanov found computable invariants by linearizing the DGA. Asking whether the DGA has a graded augmentation is a first step in generating linearized invariants:

**Definition 2.4.** An **augmentation** is an algebra map  $\varepsilon : \mathcal{A} \rightarrow \mathbb{Z}/2$  that satisfies  $\varepsilon \circ \partial = 0$  and  $\varepsilon(1) = 1$ . If, in addition, the augmentation vanishes on generators of nonzero degree, then it is **graded**.

It is easy to extend a graded augmentation over a stabilization: simply send both  $\beta$  and  $\alpha$  to 0. In the case of a degree 0 stabilization, there is another possible extension:

$$\varepsilon(\beta) = 1 \text{ and } \varepsilon(\alpha) = 0.$$

That is, if  $|\beta| = 0$ ,  $\varepsilon(\beta)$  can be either 0 or 1. Thus, Theorem 2.3(3) implies:

**Corollary 2.5.** *The existence of a graded augmentation is invariant under Legendrian isotopy.*

*Example.* The DGA for the trefoil knot in the previous example has five augmentations. For grading reasons, all of the augmentations are zero on  $q_4$  and  $q_5$ , and it is easy to check that the following assignments work:

	$q_1$	$q_2$	$q_3$
$\varepsilon_1$	1	0	0
$\varepsilon_2$	1	1	0
$\varepsilon_3$	1	1	1
$\varepsilon_4$	0	1	1
$\varepsilon_5$	0	0	1

**2.3. Rulings.** The other object involved in Theorem 1.2 is a (graded) normal ruling. To define it, suppose that a Legendrian knot  $K$  has a front diagram whose singular values all have distinct  $x$  coordinates. A **ruling** of such a front diagram of  $K$  consists of a one-to-one correspondence between the set of left cusps and the set of right cusps and, for each pair of corresponding cusps, two paths in the front diagram that join them. The ruling paths must satisfy the following conditions:

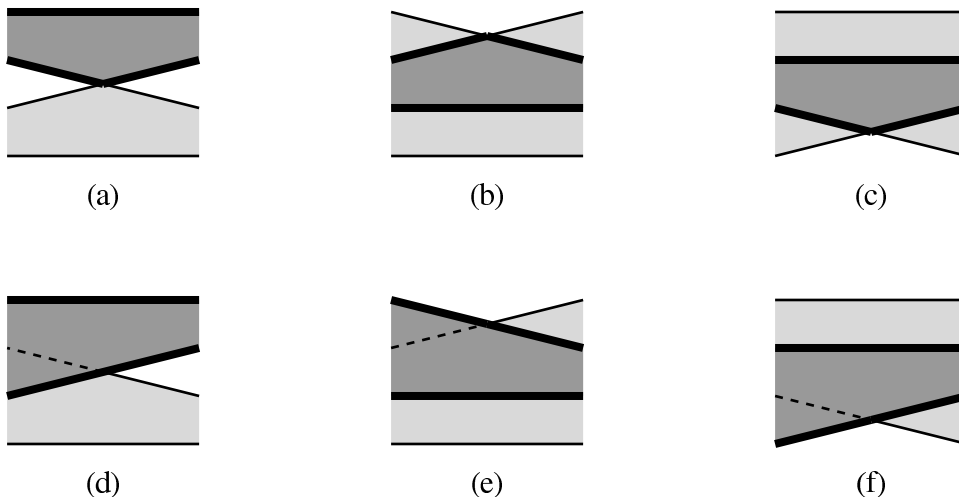


FIGURE 4. The possible configurations of a normal ruling near a crossing. Only the crossing paths and their companions are shown. Reflections of configurations (d–f) through a vertical axis are also allowed.

1. Any two paths in the ruling meet only at crossings or at cusps; and
2. The interiors of the two paths joining corresponding cusps are disjoint, and hence they meet only at the cusps and bound a topological disk. Note that these disks are similar to those used to define the differential  $\partial$ , but they may have “obtuse” corners; see Figure 4(b), for example.

As Fuchs notes, these conditions imply that the paths cover the front diagram and the  $x$  coordinate of each path in the ruling is monotonic.

At a crossing, either the two ruling paths incident to the crossing pass through each other or one path lies entirely above the other. In the latter case, say that the ruling is **switched** at the crossing. Near a crossing, call the two ruling paths that intersect the crossing **crossing paths** and the ruling paths that are paired with the crossing paths **companion paths**. If all of the switched crossings of a ruling are of types (a–c) in Figure 4, then the ruling is **normal**. If all of the switched crossings have grading 0, then the ruling is **graded**. It is not hard to see that both crossing paths have the same Maslov index in configurations (a–c), as do the companion paths in configurations (b) and (c).

*Example.* The trefoil pictured in Figure 1 has exactly three graded normal rulings. They are pictured in Figure 5.

The following theorem of Chekanov shows that graded normal rulings are interesting objects in Legendrian knot theory:



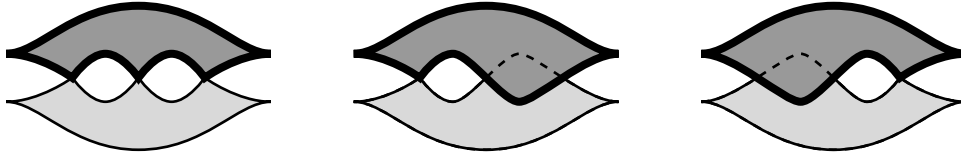


FIGURE 5. The three rulings of the trefoil knot in Figure 1.

**Theorem 2.6** (Chekanov [3]). *The number of graded normal rulings<sup>4</sup> is invariant under Legendrian isotopy.*

### 3. FROM AUGMENTATION TO RULING

The proof that the existence of an augmentation implies the existence of a ruling (Theorem 1.2) starts by constructing the beginnings of ruling paths at the left cusps and then extending them crossing by crossing to the right. The extension procedure will produce only (graded) normal switches, so the challenge will be to prove that the paths paired in the ruling match at right cusps. To do this, the proof adopts Fuchs’ philosophy of using Legendrian isotopy to simplify the differential at the expense of expanding the number of generators. In [11], Fuchs used “splashes” to prove Theorem 1.1; the proof here will use “dipped diagrams” in which the ruling and augmentation are closely related (see Section 3.1). By tracing the original augmentation through the stable tame isomorphisms that relate the DGAs of the original diagram and of the dipped diagram (see Section 3.2), it will be possible to use properties of the augmentation of the dipped diagram to conclude that the ruling paths match at the right cusps (see Section 3.3).

Since both the existence of an augmentation (Corollary 2.5) and the number of rulings (Theorem 2.6) are invariant under Legendrian isotopy, the proof of Theorem 1.2 only needs to consider Lagrangian diagrams that come from morsifying plats.

**3.1. Dipped Diagrams.** The modification of the Lagrangian diagram that simplifies the differential is called a **dip**. A dip in a plat diagram looks innocent in the front projection: it appears as the small wiggles pictured in Figure 6(a). The new front is clearly isotopic to the original one. The Lagrangian diagram, however, has changed dramatically; see Figure 6(b).

To see the transition to the dipped diagram in the Lagrangian projection in terms of Reidemeister moves, start by numbering the strands from bottom to top. Push strand  $k$  over strand  $l$  ( $k > l$ ) in ascending lexicographic order, e.g. 3 crosses 2 after 3 crosses 1, and 4 crosses 1 after 3 crosses 2. For a plat with  $c$  left cusps — and hence  $2c$  strands — this gives  $c(2c - 1)$  type II moves. The new generators for the modified diagram are simple to describe:

<sup>4</sup>Chekanov calls them **admissible decompositions** in [3]; Chekanov and Pushkar call them **positive involutions** in [4].

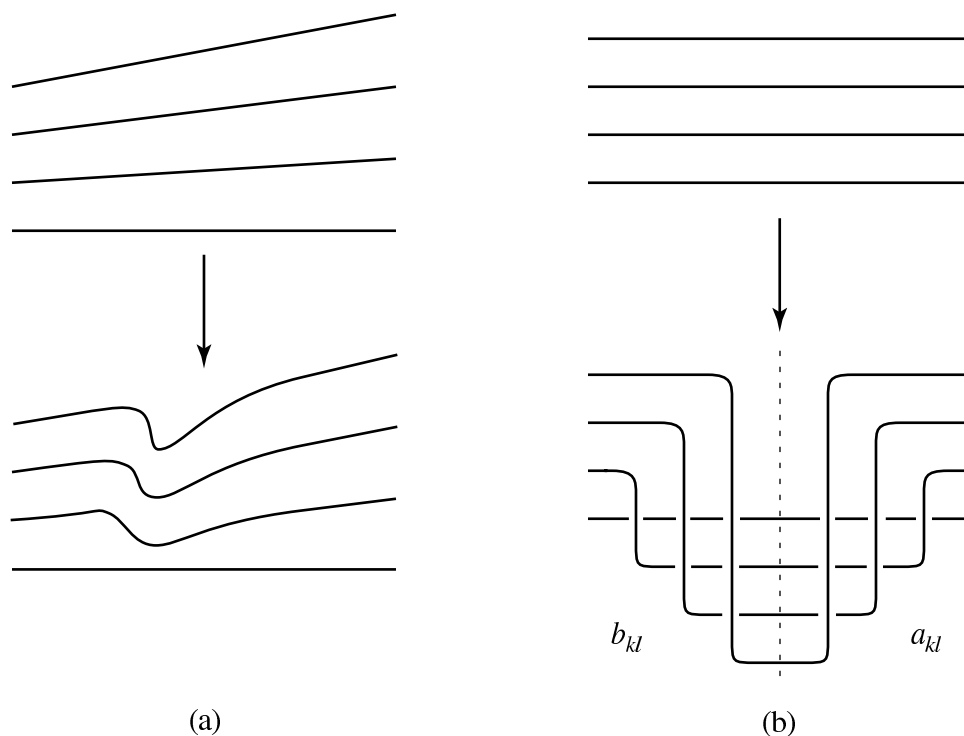


FIGURE 6. (a) The modification in the front projection; (b) The modification in the Lagrangian projection (after a small planar isotopy).

assuming  $k > l$ , denote by  $b_{kl}$  the leftmost crossing of the strands  $k$  and  $l$  and by  $a_{kl}$  the rightmost crossing.

It is not hard to check that all stages of the dipping procedure preserve the embeddedness and connected vertical slice properties of disks in plat diagrams. Of particular importance in the next few sections will be a configuration in which a crossing in a plat diagram is surrounded by dips. The general forms of the disks that give  $\partial a_{kl}$  and  $\partial b_{kl}$  for the generators in the right-hand dip are simple to describe in this situation. The disks in  $\partial a_{kl}$  lie entirely within the “half-lattice” on the right side of Figure 6(b); look ahead to Figure 9 to see an example. Some disks in  $\partial b_{kl}$  start in the right-hand dip and extend to the left-hand dip, with corners at an  $a_{kl}$  generator in the left-hand dip and possibly at the crossing and at another  $b_{kl}$  generator in the right-hand dip; look ahead to Figure 8. There are also disks that stay within a dip, with a positive corner at a  $b_{kl}$  crossing and negative corners at an  $a_{kl}$  crossing and another  $b_{kl}$  crossing, but these will play no direct role in the proof.

**3.2. Type II Moves and DGA Maps.** In order to understand how the augmentations before and after a dip are related, a closer examination of the

stable DGA isomorphism induced by a type II move is necessary. Suppose that  $(\mathcal{A}', \partial')$  is the DGA for a knot diagram before a type II move and that  $(\mathcal{A}, \partial)$  is the DGA afterward. As shown in [2], the type II move gives rise to a DGA isomorphism

$$\psi : (\mathcal{A}, \partial) \rightarrow S(\mathcal{A}', \partial').$$

In particular, note that this map preserves grading. If  $a$  and  $b$  are the two new generators that appear during a type II move, then the first step in defining  $\psi$  is to order the generators of  $\mathcal{A}$  by height: let  $\{x_1, \dots, x_N\}$  denote generators of height less than that of  $a$  in increasing height order and let  $\{y_1, \dots, y_M\}$  denote generators of height greater than that of  $b$  in increasing height order. Note that, since  $\partial$  lowers height,  $\partial y_j$  does not contain any generators  $y_k$  with  $k \geq j$ .

During the creation of a dip in a plat diagram, this ordering takes on the following form. Suppose the strand  $k$  is pushed over strand  $l$ . Each  $x_j$  either lies to the left of the dip, or  $x_j = a_{ij}$  or  $b_{ij}$  with  $i - j \leq k - l$ . Similarly,  $y_j$  either lies to the right of the dip, or  $y_j = a_{ij}$  or  $b_{ij}$  with  $i - j > k - l$ .

The definition of the map  $\psi$  needs a *vector space* map  $H$  defined on  $S(\mathcal{A}')$  by:

$$H(w) = \begin{cases} 0 & w \in \mathcal{A}' \\ 0 & w = Q\beta R \quad \text{with } Q \in \mathcal{A}' \\ Q\beta R & w = Q\alpha R \quad \text{with } Q \in \mathcal{A}'. \end{cases}$$

Also write  $\partial b = a + v$ , where  $v$  is a sum of words consisting entirely of the letters  $x_1, \dots, x_N$ . Inductively define maps  $\psi_i$  on the generators of  $\mathcal{A}$  by:

$$\psi_0(w) = \begin{cases} \beta & w = b \\ \alpha + v & w = a \\ w & \text{otherwise.} \end{cases}$$

and

$$\psi_i(w) = \begin{cases} y_i + H\psi_{i-1}(\partial y_i) & w = y_i \\ \psi_{i-1}(w) & \text{otherwise.} \end{cases}$$

That the resulting map  $\psi = \psi_M$  is a DGA isomorphism between  $\mathcal{A}$  and  $S(\mathcal{A}')$  was proven in [2].<sup>5</sup>

If there is an augmentation  $\varepsilon'$  on  $S(\mathcal{A}')$ , then  $\varepsilon = \varepsilon'\psi$  is an augmentation on  $\mathcal{A}$ . It is straightforward to see that  $\varepsilon(x_j) = \varepsilon'(x_j)$  and that:

$$(4) \quad \varepsilon(b) = \varepsilon'(\beta) \text{ and } \varepsilon(a) = \varepsilon'(v).$$

Recall that if  $|\beta| = 0$ , then  $\varepsilon'(\beta)$  may be chosen arbitrarily. Though the procedure is complicated in general, in a plat diagram, there is a simple inductive condition to determine if  $\varepsilon$  will differ from  $\varepsilon'$  on a generator  $y_j$ :

<sup>5</sup>This appears to be slightly different from the map given in [2, 10]; it is not hard to check, however, that the definition is equivalent.

**Lemma 3.1.** *After a type II move involved in making a dip in a plat diagram, suppose that  $\varepsilon(y_i)$  has been determined for all  $i < j$ . Then  $\varepsilon'(y_j) \neq \varepsilon(y_j)$  if and only if  $\varepsilon'(\beta) = 1$  and there exists an odd number of terms in  $\partial y_j$  that are of the form  $QaR$ , where  $Q, R \in \mathcal{A}'$ ,  $\varepsilon'(Q) = 1$  and  $\varepsilon(R) = 1$ .*

*Proof.* Since

$$(5) \quad \psi(y_j) = y_j + H\psi(\partial y_j),$$

the augmentations  $\varepsilon$  and  $\varepsilon'$  disagree on  $y_j$  if and only if  $\varepsilon'(H\psi(\partial y_j)) \neq 0$ . The proof that the latter is equivalent to the second condition in the lemma proceeds by induction on  $j$ .

For  $j = 1$ , write

$$(6) \quad \partial y_1 = P + \sum_k Q_k a R_k$$

where  $Q_k \in \mathcal{A}'$  and for every term in  $P$  that contains  $a$ , there is a  $b$  that precedes  $a$ . The paragraph at the end of Section 3.1 implies that all terms in  $\partial y_1$  contain at most one  $a$ , so  $a$  appears only where indicated in (6). Since the differential lowers height,  $P$ ,  $Q_k$ , and  $R_k$  lie in the algebra generated by  $\{x_1, \dots, x_N, b\}$ . It follows that:

$$\begin{aligned} H\psi(\partial y_1) &= H(\psi(P) + \sum_k Q_k(\alpha + v)\psi(R_k)) \\ &= \sum_k Q_k \beta \psi(R_k), \end{aligned}$$

since  $Q_k \alpha \psi(R_k)$  is the only term that has an  $\alpha$  before any  $\beta$ s that might exist. The lemma follows in this case. This argument also shows that  $\alpha$  does not appear in  $\psi(y_1)$ .

In general, write out  $\partial y_j$  as in equation (6). As before, the generator  $a$  only appears where indicated, and  $Q_k$  lies in the algebra generated by  $\{x_1, \dots, x_N, y_1, \dots, y_{j-1}\}$ . Inductively,  $\psi(y_i)$  does not contain  $\alpha$  for  $i < j$ , so the images of  $Q_k$  and  $R_k$  under  $\psi$  do not contain  $\alpha$ . Further, the image  $P$  under  $\psi$  does not contain a term in which  $\alpha$  precedes  $\beta$ . Computing as before, using the facts about the images of  $P$ ,  $Q_k$ , and  $R_k$ ,

$$(7) \quad H\psi(\partial y_j) = \sum_k Q_k \beta \psi(R_k).$$

Once again, this implies that  $\alpha$  does not appear in  $\psi(y_j)$ , so this fact may be used inductively. The lemma follows from (5) and (7).  $\square$

**3.3. Extension of the Ruling.** Using knowledge of the dipping modifications and their relationship with augmentations, the heart of the proof of Theorem 1.2 extends ruling paths that start at a common left cusp over successive crossings to the right. The extension procedure has three parts:

1. Extend the ruling over  $q_j$ ;
2. Place a dip between  $q_j$  and  $q_{j+1}$ ; and

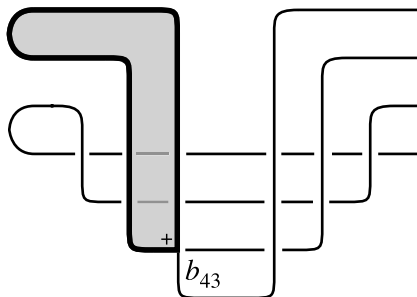


FIGURE 7. The dip next to the left cusp with an augmented disk in  $v_{43}$ .

3. Construct an augmentation  $\varepsilon_{j+1}$  on the DGA of the newly dipped diagram.

The augmentations  $\varepsilon_{j+1}$  will have the following property:

**Property (R).** At any dip,  $a_{kl}$  is augmented if and only if the strands  $k$  and  $l$  are paired in the ruling between  $q_j$  and  $q_{j+1}$ .

In more detail, the extension proceeds as follows. In a the Lagrangian projection that comes from morsifying a plat diagram, label the crossings that correspond to crossings of the plat by  $q_1, \dots, q_n$ . At the left cusps, any ruling must pair paths incident to the same cusp. The next step is to analyze the behavior of the augmentation  $\varepsilon$  during the construction of a dip between the left cusps and  $q_1$ . Consider the type II move that pushes strand  $k$  over strand  $l$ . Choose  $\varepsilon'(\beta) = 0$ . It follows from equation (4) that  $\varepsilon_1(b_{kl}) = 0$  for all  $k$  and  $l$ . Further, equation (4) and Lemma 3.1 imply that  $a_{kl}$  is augmented only if the corresponding  $v_{kl}$  is. Using the fact that  $\varepsilon_1(b_{kl}) = 0$  for all  $k$  and  $l$ , a quick examination of Figure 7 shows that  $v_{kl}$  is augmented only when  $k$  and  $l$  are incident to the same left cusp. It follows that  $\varepsilon_1$ , the augmentation on the diagram after the construction of the dip, satisfies property (R).

At the crossing  $q_j$ , extend the ruling paths as follows: if  $\varepsilon_j(q_j) = 1$  and the ruling to the left of  $q_j$  matches the situation in configurations (a), (b), or (c) in Figure 4, then there is a switch at  $q_j$ . Otherwise, there is no switch. By construction, the ruling paths have only (graded) normal switches.

As above, the next step is to understand the augmentation  $\varepsilon_{j+1}$  that results from the construction of a dip between  $q_j$  and  $q_{j+1}$ . There is a choice of augmentation on the  $\beta$  generators; the goal is to make choices that will lead to  $\varepsilon_{j+1}$  satisfying property (R) if  $\varepsilon_j$  does. The exact choice of augmentations depends on  $\varepsilon_j(q_j)$  and the configuration of the ruling near the crossing  $q_j$ ; each configuration will be examined separately.

**Any configuration when  $\varepsilon_j(q_j) = 0$ :** For every type II move in the dip, extend  $\varepsilon_j$  so that  $\varepsilon_j(\beta) = 0$ . The ruling is *not* switched in these configurations. As at the left cusps, Lemma 3.1 implies  $\varepsilon_{j+1}(a_{kl}) = \varepsilon_j(v_{kl})$ . A term in  $v_{kl}$  is augmented only if its corresponding disk ends

at an augmented  $a$  generator in the dip to the left of  $q_j$  and has no other corners. Thus, since  $\varepsilon_j$  satisfies property (R), the augmented disks in  $v_{kl}$  follow the ruling paths across  $q_j$  and hence have positive corners that involve strands paired in the ruling. It follows that  $\varepsilon_{j+1}$  also satisfies property (R).

Note that in all subsequent cases,  $\varepsilon_j(q_j) = 1$ .

**Configuration (a):** Extend  $\varepsilon_j$  so that  $\varepsilon_j(\beta) = 0$  except in the case when one crossing strand is pushed over the other. A straightforward generalization of Lemma 3.4 of [10] shows that if there exists a disk with two positive corners, one at  $x$  and one at  $y$ , then  $|x| = |y|$ . Since such a disk exists with corners at  $b$  and  $q_j$  when the crossing strands are involved in a type II move,  $b$  and  $q_j$  must have the same grading. Since  $\varepsilon_j(q_j) = 1$ , it must be true that  $|q_j| = 0$ , so  $|b| = 0$  and hence it is possible to choose  $\varepsilon_j(\beta) = 1$  in a graded augmentation.

To determine the augmentations of the generators  $a_{kl}$ , first consider the contribution to  $\varepsilon_{j+1}(a_{kl})$  from  $\varepsilon_j(v_{kl})$ . If a disk in  $v_{kl}$  is augmented, then its leftmost corner must involve strands that are paired in the ruling. Unless one of  $k$  or  $l$  is a crossing strand, property (R) follows by the same argument as in the first case. If, on the other hand, one of  $k$  or  $l$  is a crossing strand, then there are precisely five disks with augmented negative corners; see Figure 8. If the companion strands are denoted by  $K$  and  $L$  ( $K > L$ ), then these disks show that the  $v_{kl}$  terms contribute nontrivially to the augmentations of  $a_{K,i+1}$ ,  $a_{i,L}$ ,  $a_{i+1,L}$ , and no other  $a_{kl}$  that involves a crossing strand (the two disks ending at  $b_{K,i}$  cancel).

The fact that the augmentation of  $a_{i+1,L}$  has a nonzero contribution would seem to contradict property (R). Consider, however, the type II move between the crossing strands  $i$  and  $i+1$ . Note that since  $i > L$  in this case, this move comes after the move involving strands  $i+1$  and  $L$ . The disk in Figure 9 that appears after strand  $i+1$  has been pushed over strand  $i$  contributes the term  $a_{i+1,i}a_{i,L}$  to  $\partial(a_{i+1,L})$ . If  $\varepsilon'$  is the augmentation before strand  $i+1$  has been pushed over strand  $i$  and  $\varepsilon$  is the augmentation after, the computations above using  $v_{i,L}$  show that  $\varepsilon(a_{i,L}) = 1$ . Lemma 3.1 then implies that  $\varepsilon'(a_{i+1,L}) \neq \varepsilon(a_{i+1,L})$ . Since  $\varepsilon'(a_{i+1,L}) = 1$ , it follows that  $\varepsilon(a_{i+1,L}) = 0$ . Since this is the only disk that has a negative corner at  $a_{i+1,i}$  and whose other corners are augmented, Lemma 3.1 implies that this is the only correction to the augmentation. Thus, the only augmented  $a$  generators that involve the crossing strands are  $a_{K,i+1}$  and  $a_{i,L}$ ; this is exactly what property (R) requires.

**Configurations (b) and (c):** Extend  $\varepsilon_j$  so that exactly two  $\beta$  generators are augmented: the crossing of the crossing strands and the crossing of the companion strands. The argument that these choices work is entirely similar to that of configuration (a).

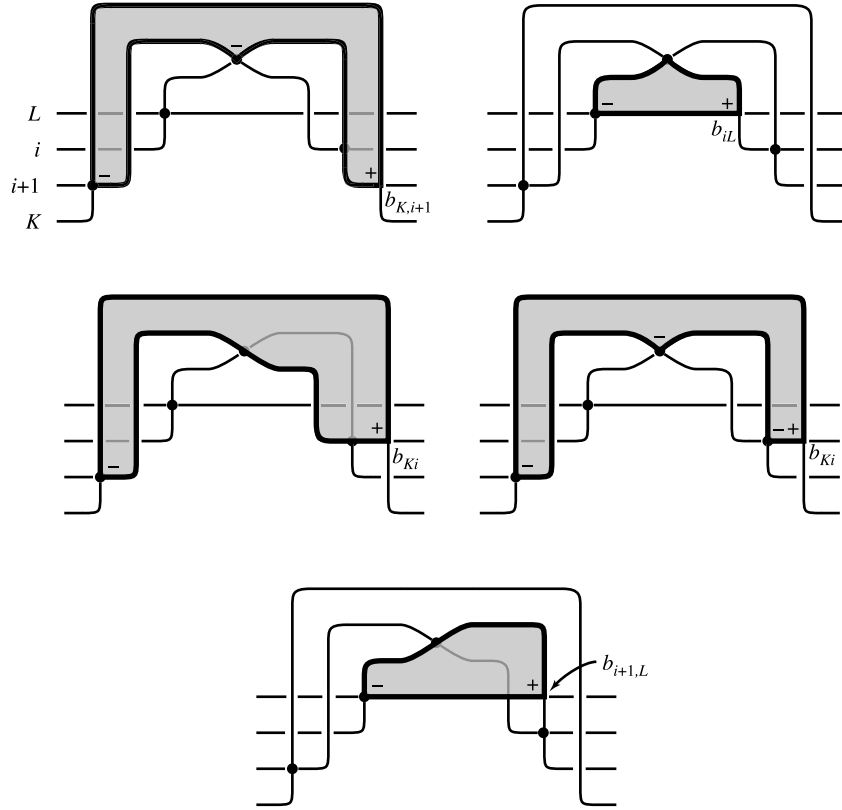


FIGURE 8. The five disks in configuration (a) that contribute to the augmentation  $\varepsilon_{j+1}$ . The disks in the top row give the augmentations that are necessary for property (R); the disks in the second row cancel; and the disk in the bottom row gets corrected by the disk in Figure 9. Dots indicate augmented crossings.

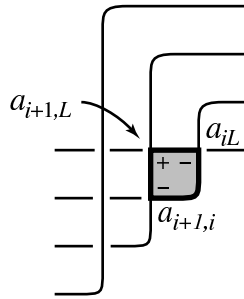


FIGURE 9. The disk that corrects the augmentation in configuration (a) so that it satisfies property (R).

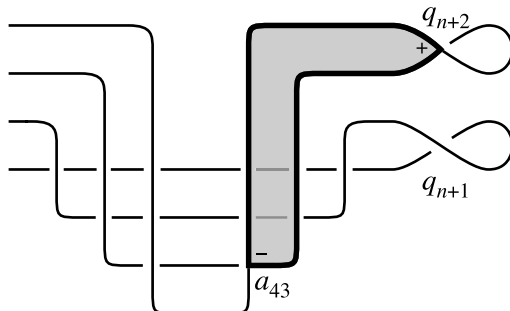


FIGURE 10. The dip next to the right cusp with the disk that gives the  $a_{21}$  term in  $\partial q_{n+1}$ .

**Configuration (d):** For every type II move, extend  $\varepsilon_j$  so that  $\varepsilon_j(\beta) = 0$ .

The argument for property (R) is similar to that of the case when  $\varepsilon_j(q_j) = 0$ .

**Configurations (e) and (f):** Extend  $\varepsilon_j$  so that the only augmented  $\beta$  generator corresponds to the crossing of the companion strands. The argument in this case is similar to that of configuration (a), though configuration (e) does not have any corrective disks.

Since  $\varepsilon_1$  satisfies property (R), the argument above shows that  $\varepsilon_n$  does as well. The proof of Theorem 1.2 will be complete if the paired ruling paths match at the right cusps. This holds true if and only if, in the dip just to the left of the right cusps,  $a_{2k,2k-1}$  is augmented for  $k = 1, \dots, c$ . As shown in Figure 10, the differential of the  $k^{\text{th}}$  right cusp in the dipped diagram is:

$$\partial q_{n+k} = 1 + a_{2k,2k-1}.$$

Since  $\varepsilon_n$  is a genuine augmentation, this implies that  $a_{2k,2k-1}$  is augmented. Theorem 1.2 follows since  $\varepsilon_n$  obeys property (R).

*Remark.* The proof can be refined to give an algorithm for constructing a ruling from the augmentation, and can even be carried out without passing to the dipped diagram. As in the proof, the idea is to extend the ruling over a crossing  $q_j$  given the value  $\varepsilon_j(q_j)$ . Before, it was not necessary to explicitly find these values, but it is possible to determine them.

The key to finding  $\varepsilon_j(q_k)$  for  $k > j$  is Lemma 3.1. Disks of the form  $QaR$ , where  $Q, R \in \mathcal{A}'$ , appear in the original plat as disks with a positive corner at  $q_k$ , negative corners at  $Q$  and  $R$ , and a line segment to the right of  $q_j$  that joins the crossing strands (if the  $\beta$  generator at the crossing is augmented) or the companion strands (if the corresponding  $\beta$  generator is augmented); see Figure 11. The value of  $\varepsilon_j(q_k)$  differs from that of  $\varepsilon_{j+1}(q_k)$  if there is an odd number of these disks with  $\varepsilon_j(Q) = 1$  and  $\varepsilon_{j+1}(R) = 1$ . If two  $\beta$  generators are augmented, then the procedure should be performed once for each  $\beta$  with the  $\beta$  between the lower-numbered strands going first.

Figure 12 demonstrates the procedure on the trefoil with the augmentation  $\varepsilon_3$  that marks all three crossings of degree 0. Note that all of the disks



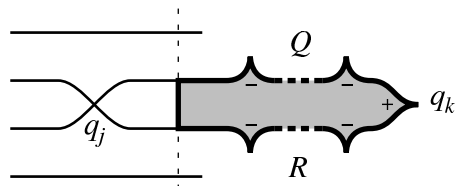


FIGURE 11. A schematic picture of a disk that contributes to changing  $\varepsilon_{j+1}(q_k)$  in configuration (a).

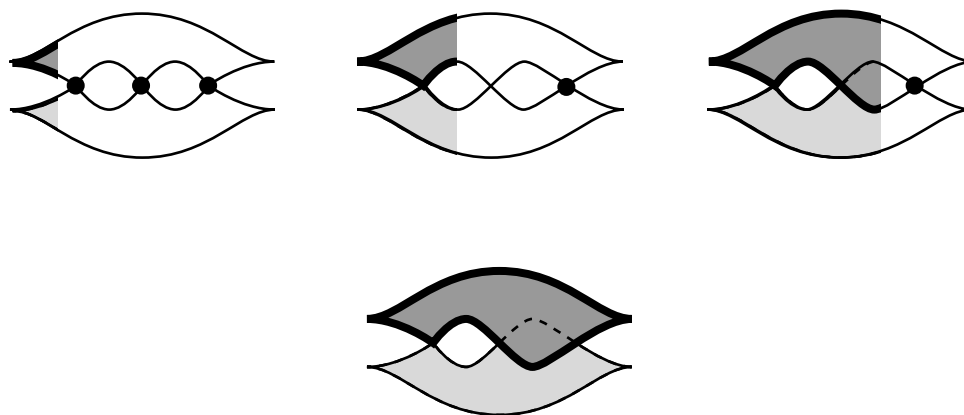


FIGURE 12. The result of carrying out the procedure in this section on the trefoil with the augmentation  $\varepsilon_3$  that sends all three crossings of degree 0 to 1.

involved in adjusting the augmentation have no negative corners, so  $Q$  and  $R$  are always 1 in Lemma 3.1, and the condition is easy to apply.

#### 4. ROTATION NUMBER AND RULINGS

This section contains the proof of Theorem 1.3. Before beginning the proof, a note about gradings of DGAs for Legendrian links is in order. If a link has  $n$  components, then the Maslov index  $\mu$  is well-defined up to a choice of  $n$  constants. The grading for the generators of a link DGA therefore are only well-defined up to a choice of  $n - 1$  constants.<sup>6</sup> What those constants are do not matter for the following proof; only the idea that a Maslov index still gives a grading on the DGA of a Legendrian link. In the proof, assume that the Maslov index takes values in  $\mathbb{Z}/2$ .

*Proof of Theorem 1.3.* By Theorem 1.2, it suffices to prove that if an oriented front diagram of  $K$  has a normal ruling where the switches all have even grading, then  $r(K) = 0$ .

<sup>6</sup>In the notation of [14], these constants are  $\rho_1, \dots, \rho_{n-1}$ .

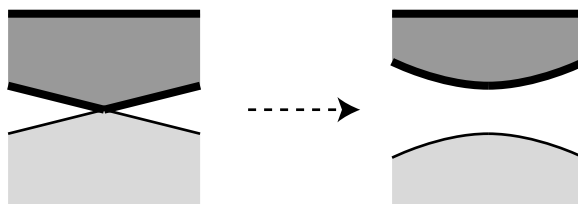


FIGURE 13. Smoothing ruling disks at a switch. The other configurations are similar.

First, notice that the strands at a switched crossing are both oriented to the left or both to the right. This implies that the boundary of a disk in a graded normal ruling inherits a coherent orientation from the knot, and hence that each disk pairs an upward (resp. downward) right cusp with a downward (resp. upward) left cusp.

The proof now proceeds by contradiction: suppose that the Legendrian knot  $K$  has nonzero rotation number and that there is a front diagram of  $K$  with a mod 2 graded normal ruling. Choose a ruling disk and smooth its switched crossings as in Figure 13. Remove the smoothed disk to leave a Legendrian link. The link's Maslov index is inherited from that of  $K$ ; this is possible since the smoothed crossings have grading 0, and hence all strands incident to the crossing have the same  $\mu$  value. This link has a graded normal ruling given by the (smoothed) ruling disks that remain from  $K$ . The observation about how graded normal ruling disks pair upward cusps with downward ones implies that the operation of removing the smoothed ruling disk does not change the total rotation number.

Repeat this procedure until there is but one right cusp remaining. In this base case, the observation above implies that the right cusp and the left cusp are pointing in opposite directions, and hence that the rotation number is zero. This contradicts the assumption that  $K$  has nonzero rotation number, and the theorem follows.  $\square$

#### REFERENCES

1. D. Bennequin, *Entrelacements et equations de Pfaff*, Asterisque **107–108** (1983), 87–161.
2. Yu. Chekanov, *Differential algebra of Legendrian links*, Invent. Math. **150** (2002), 441–483.
3. ———, *Invariants of Legendrian knots*, Proceedings of the International Congress of Mathematicians, Vol. II (Beijing, 2002) (Beijing), Higher Ed. Press, 2002, pp. 385–394.
4. Yu. Chekanov and P. Pushkar, *The combinatorics of fronts of Legendrian knots*, Preprint., 2004.
5. T. Ekhholm, J. Etnyre, and M. Sullivan, In preparation.
6. Y. Eliashberg and M. Fraser, *Classification of topologically trivial Legendrian knots*, Geometry, topology, and dynamics (Montreal, PQ, 1995), Amer. Math. Soc., Providence, RI, 1998, pp. 17–51.

7. Y. Eliashberg, A. Givental, and H. Hofer, *Introduction to symplectic field theory*, Geom. Funct. Anal. (2000), no. Special Volume, Part II, 560–673, GAFA 2000 (Tel Aviv, 1999).
8. J. Etnyre, *Legendrian and transversal knots*, To appear in the Handbook of Knot Theory, 2003.
9. J. Etnyre and K. Honda, *Knots and contact geometry*, J. Symplectic Geom. **1** (2002), no. 1, 63–120.
10. J. Etnyre, L. Ng, and J. Sabloff, *Invariants of Legendrian knots and coherent orientations*, J. Symplectic Geom. **1** (2002), no. 2, 321–367.
11. D. Fuchs, *Chekanov-Eliashberg invariant of Legendrian knots: existence of augmentations*, J. Geom. Phys. **47** (2003), no. 1, 43–65.
12. D. Fuchs and T. Ishkhanov, *Invariants of Legendrian knots and decompositions of front diagrams*, Moscow Math. J. (2004), To appear.
13. K. Fukaya and Y.-G. Oh, *Zero-loop open strings in the cotangent bundle and Morse homotopy*, Asian J. Math. **1** (1997), no. 1, 96–180.
14. L. Ng, *Computable Legendrian invariants*, Topology **42** (2003), no. 1, 55–82.
15. ———, *Knot and braid invariants from contact homology i*, Available on arXiv as math.GT/0302099, 2003.
16. L. Ng and L. Traynor, *Legendrian solid-torus links*, Available on arXiv as math.SG/0407068, 2004.
17. J. Sabloff, *Invariants for Legendrian knots from contact homology*, In preparation.
18. L. Traynor, *Generating function homology for Legendrian links*, Geom. and Top. **5** (2001), 719–760.
19. Ke Zhu, *Degeneration of the moduli space of  $j$ -holomorphic discs and legendrian contact homology*, Ph.D. thesis, Stanford University, 2004.

HAVERFORD COLLEGE, HAVERFORD, PA 19041

*E-mail address:* jsabloff@haverford.edu